

The podiform chromitites in the Dağküplü and Kavak mines, Eskişehir ophiolite (NW-Turkey): Genetic implications of mineralogical and geochemical data

I. UYSAL^{|1|} F. ZACCARINI^{|2|} M.B. SADIKLAR^{|1|} M. TARKIAN^{|3|} O.A.R. THALHAMMER^{|2|} and G. GARUTI^{|4|}

^{|1|} Department of Geological Engineering, Karadeniz Technical University
61080 Trabzon, Turkey. E-Mail: iuysal@ktu.edu.tr, uysal.ibrahim@gmail.com

^{|2|} Department of Applied Geological Sciences and Geophysics, University of Leoben
Peter Tunner St. 5, A-8700 Leoben, Austria

^{|3|} Institute of Mineralogy and Petrology, University of Hamburg
Grindelallee 48, 20146 Hamburg, Germany

^{|4|} Dipartimento di Scienze della Terra, University of Modena and Reggio Emilia
Via S. Eufemia 19, 41100 Modena, Italy

ABSTRACT

Mantle tectonites from Eskişehir (NW-Turkey) include high-Cr chromitites with limited variation of Cr#, ranging from 65 to 82. Mg# ratios are between 54 and 72 and chromite grains contain up to 3.71 wt% Fe₂O₃ and 0.30 wt% TiO₂. PGE contents are variable and range from 109 to 533 pbb. Chondrite-normalized PGE patterns are flat from Os to Rh and negatively sloping from Rh to Pd. Total PGE contents and low Pd/Ir ratios (from 0.07 to 0.41) of chromitites are consistent with typical ophiolitic chromitites. Chromite grains contain a great number of solid inclusions. They comprise mainly of highly magnesian (Mg# 95-98) mafic silicates (olivine, amphibole and clinopyroxene) and base-metal sulfide inclusions of millerite (NiS), godlevskite (Ni₇S₆), bornite (Cu₅FeS₄) with minor Ni arsenides of maucherite (Ni₁₁As₈) and orcelite (Ni_{5-x}As₂), and unnamed Cu₂FeS₃ phases. Heazlewoodite, awaruite, pyrite, and rare putoranite (Cu₉Fe,Ni₉S₁₆) were also detected in the matrix of chromite as secondary minerals. Laurite [(Ru,Os)S₂] was the only platinum-group minerals found as primary inclusions in chromite. They occur as euhedral to subhedral crystals trapped within chromite grains and are believed to have formed in the high temperature magmatic stage during chromite crystallization. Laurite has limited compositional variation, range between Ru_{0.94}Os_{0.03}Ir_{0.02}S_{1.95} and Ru_{0.64}Os_{0.21}Ir_{0.10}S_{1.85}, and contain up to 1.96 at% Rh and 3.67 at% As. Close association of some laurite grains with amphibole and clinopyroxene indicates crystallization from alkali rich fluid bearing melt in the suprasubduction environment. The lack of any IPGE alloys, as well as the low Os-content of laurite, assumes that the melt from which chromite and laurite were crystallized had relatively high fS₂ but never reached the fS₂ to crystallize the erlichmanite. The presence of millerite, as primary inclusions in chromite, reflects the increasing fS₂ during the chromite crystallization.

KEYWORDS | Chromite. Platinum-group minerals. Platinum-group elements. Eskişehir ophiolite. Turkey

INTRODUCTION

Chromium is an essential economic element with a wide range of industrial applications in metallurgy (e.g. corrosion resistency, stainless steel), in the refractory industry, glass industry, used as a catalyst etc., and finds also application as a strategic element in the military industry (e.g. “superalloy”). Chromite represents a significant economic resource for Turkey, where about 2000 deposits of chromitites have been recognized so far, and Turkey ranks among the big chromium producers in the world, apart of Kazakhstan and South Africa. Most of the Turkish chromitites are of the podiform-type and occur in the mantle sequence of ophiolite complexes. Furthermore, it is commonly known, today, that podiform chromitites may contain economic concentrations of platinum group elements (PGE) with particular enrichment of Ru, Os and Ir (i.e. the IPGE), the reason why podiform chromitites may be considered a potential target for IPGE recovery (Economou-Eliopoulos, 1993, 1996; Economou-Eliopoulos and Vacondios, 1995; Kostantopoulou and Economou-Eliopoulos, 1991; Melcher et al., 1997; Ahmed and Arai, 2002; Distler et al., 2008).

In the last decades, it has been demonstrated that the compositional characteristics of chromite, its solid and fluid inclusions, as well as the PGE mineralogy and geochemistry can be successfully used to obtain information on the genesis of the particular ophiolite complex, its geotectonic setting, and the chemical-physical conditions prevailing in the mantle during ophiolite formation (Thalhammer et al., 1990; Melcher et al., 1997; Garuti et al., 1999; Malitch et al., 2003; Uysal et al., 2005, 2007a, b; Kocks et al., 2007; Proenza et al., 2008; Zaccarini et al., 2008).

In this paper we present, for the first time, a detailed investigation of the podiform chromitites collected in the Dağköplü and Kavak mines located in the Eskişehir ophiolite (NW Turkey). Very limited data on these chromitites were available so far, restricted to a description of the chromium ore (Rechenberg, 1960; Eskikaya and Aydinler, 2000) and to some processing technique (Beklioglu and Arol, 2004). The present study is based on the mineralogy and geochemistry of chromite, its solid inclusions, on the associated silicate phases, and the PGE. The obtained data are used to elucidate the origin of the Dağköplü and Kavak chromitites, their tectonic setting, and an evaluation of the economic potential.

SIMPLIFIED GEOLOGY AND PETROGRAPHY OF ESKIŞEHİR OPHIOLITE AND DESCRIPTION OF THE INVESTIGATED CHROMITITE

The Eskişehir ophiolite is located in the western part of “Izmir-Ankara-Erzincan Suture Zone (IAESZ)” which

trends from the northern part of Izmir eastwards to the border with Georgia and marks the opening of the Tethys ocean between Laurasia and Gondwana (Şengör, 1987). The formation of the Eskişehir ophiolite is related to subduction and obduction processes caused by the collision of the Sakarya Continent and the Anatolide Platform (Fig. 1A) and consequently the subsequent closure of the northern branch of the Neotethyan Ocean in Late Cretaceous-Paleocene times (Sarifakioglu, 2007).

The Eskişehir ophiolite is composed of mafic-ultramafic rocks that are considered remnants of the oceanic lithosphere, accompanied by an ophiolitic mélange that comprises oceanic and continental fragments. Although the Eskişehir ophiolite consists of dismembered fragments, displaying an incomplete and inverted ophiolite suite, the following units have been recognized: 1) a restitic mantle, consisting predominantly of harzburgite and minor dunite, cut by diabase dyke swarms up to 75 cm thick; 2) a cumulus pile, made up of dunite, wehrlite, pyroxenite, massive to layered gabbros and minor gab-

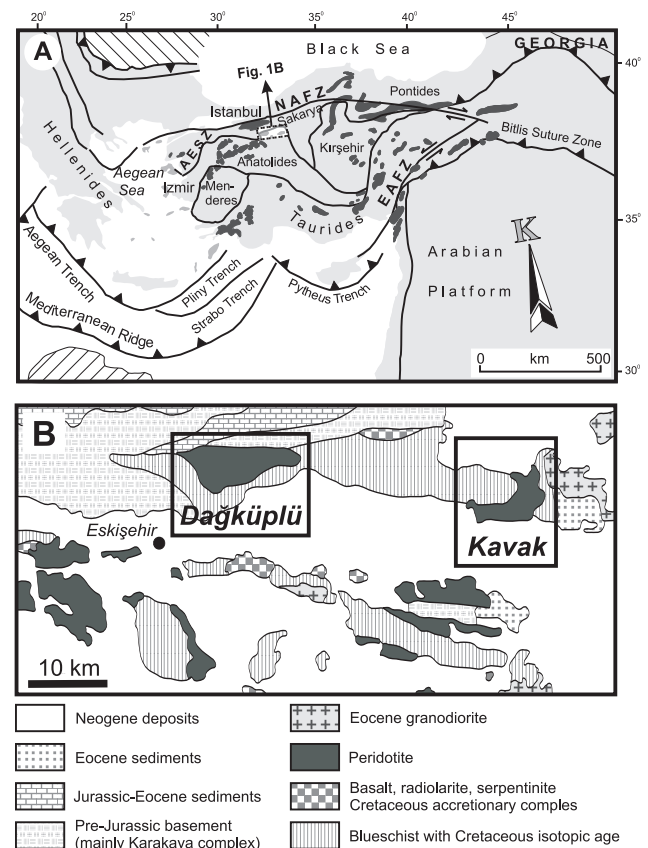


FIGURE 1 | **A)** Distribution of the major ophiolite complexes on a map showing the major blocks of Turkey. NAFZ: North Anatolian Fault Zone, EAFZ: Eastern Anatolian Fault Zone; IAESZ: Izmir-Ankara-Erzincan Suture Zone. **B)** Simplified geological map of Eskişehir area (modified from Okay, 1984). Insets in B show chromitite sample locations in the Dağköplü and Kavak mines.

bronorite, 3) a sheeted dyke complex, and 4) dykes of plagiogranites cutting across cumulate gabbro and sheeted dyke complex (Sarifakioglu, 2007).

Mantle harzburgite, composed of olivine, orthopyroxene (enstatite), and trace amount of clinopyroxene with accessory chromite, represents the most abundant rock in the Eskişehir ophiolite. The mantle harzburgite is moderately to sometimes completely serpentinized and contains podiform chromitites typically enveloped by dunite. These chromitites are mined locally.

The chromitites investigated were collected in the Dağköplü and Kavak mines (Fig. 1B) and represent disseminated, banded, and nodular textures. The matrix of chromite is composed mainly of serpentine as well as minor olivine and, base-metal sulfide and alloy minerals. The boundaries of the chromitite pods with enclosing dunite are generally sharp, but diffuse in some deposits. The mining activity at Dağköplü has ceased, whereas the Kavak mine is still in operation. According to Eskişaya and Aydiner (2000) the Kavak mine has 2 million tons of ore reserves, with an annual production of about 100,000 tons. The Kavak chromitites display massive, disseminated and banded textures.

METHODOLOGY

Identification of mineral phases and textural relationships of PGM, base-metal phases and silicate inclusions in chromite were investigated microscopically on polished thick and thin sections under reflected light at 250 to 500-times magnifications.

Microprobe analyses were carried out using a CAMECA SX-100 wavelength dispersive electron-probe micro-analyzer (EPMA) at the Institute of Mineralogy and Petrology, University of Hamburg, Germany. Analytical conditions for quantitative WDS analyses were 15-20 kV accelerating voltage, 20 nA beam current at a beam diameter of 1 μm , and counting times of 20 s per element. Calibrations were performed using natural and synthetic reference materials of andradite for Ca, Si, Fe, corundum for Al, periclase for Mg, rutile for Ti, albite for Na, orthoclase for K, chromite for Cr and NiO for Ni. Fe^{2+} and Fe^{3+} contents of the Cr-spinels were calculated on the basis of spinel stoichiometry (XY_2O_4). Pure metals were used as standards for PGE, Ni and Cu, arsenopyrite for As and pyrite for Fe. The following X-ray lines were used in the analyses: $\text{L}\alpha$ for Ru, Ir, Rh, Pt, $\text{M}\alpha$ for Os, $\text{L}\beta$ for Pd, As and $\text{K}\alpha$ for S, Ni, Fe, and Cu.

Chromitite samples were analyzed for all PGE using the nickel sulfide fire-assay pre-concentration technique, followed by ICP-MS at Genalysis Laboratory, Perth,

Western Australia. Detection limits were 2 ppb for Os, Ir, Ru, Pt, Pd, 1 ppb for Rh and 5 ppb for Au. The internal standards SARM7b for all PGE and Au were used.

MINERAL CHEMISTRY

Composition of chromite and associated minerals

The chromite of the Dağköplü and Kavak chromitites exhibits moderate alteration to ferrian-chromite along grain boundaries and related to cracks. However, the major core portion of the chrome spinel is fresh and this was used for microprobe analyses. Selected analyses of chromite are shown in Table 1 (see Appendix). Chromite composition is characterized by Cr_2O_3 ranging from 63.29 to 51.03 wt.%, Al_2O_3 from 18.27 to 9.28 wt.%, MgO 15.34 to 11.25 wt.%, and FeO ranges from 17.1 to 10.7 wt.%. The maximum Fe_2O_3 content is 3.71 wt% and TiO_2 is always below 0.3 wt%, as typical for podiform chromitites. The Cr# [$100\text{Cr}/(\text{Cr}+\text{Al})$] ratio ranges from 65 to 82 and the Mg# [$100\text{Mg}/(\text{Mg}+\text{Fe}^{2+})$] lies between 54 and 72. Chromite from Dağköplü shows a wider range of Cr content (Fig. 2).

The compositional characteristics of the Dağköplü and Kavak chromites, i.e. Cr, Al, Mg, Fe^{3+} and Ti concentrations, are in accordance with those from typical podiform chromitites hosted in the mantle section of ophiolites. Their composition definitely differ from stratiform chromitites, such as those in Precambrian continental layered intrusions, as shown in Fig. 2A, B.

Fe-Mg exchange temperatures (Ballhaus et al., 1991) of chromite from massive chromitite and olivine from coexisting silicate mantle dunite or harzburgite ($\text{Fo} \sim 92$) are between 915 and 1200°C, which suggests magmatic origin of chromite. Calculated oxygen fugacities are between -8.05 and -11.74, decreasing with temperature along a T-fO₂ trend that is near and parallel to the FMQ reaction line. These fugacities are similar to those measured in ophiolitic chromitites from the Urals and much lower than those of Uralian-Alaskan type complexes (Fig. 3).

Composition of solid inclusions in chromites

Chromite from Dağköplü and Kavak chromitites contains solid inclusions of silicates and base-metal sulfides, accompanied by minor arsenides and alloys. They generally form mono-phase inclusions, varying in size from 5 up to 100 μm . On the basis of their euhedral shapes and their homogeneous unaltered chromite host, many of these inclusions are considered as primary, i.e. formed at high temperature, concomitantly with the crystallization of the host chromites. Selected optical images of primary

silicate inclusions are shown in Fig. 4. Other inclusions are undoubtedly secondary with respect to chromite for-

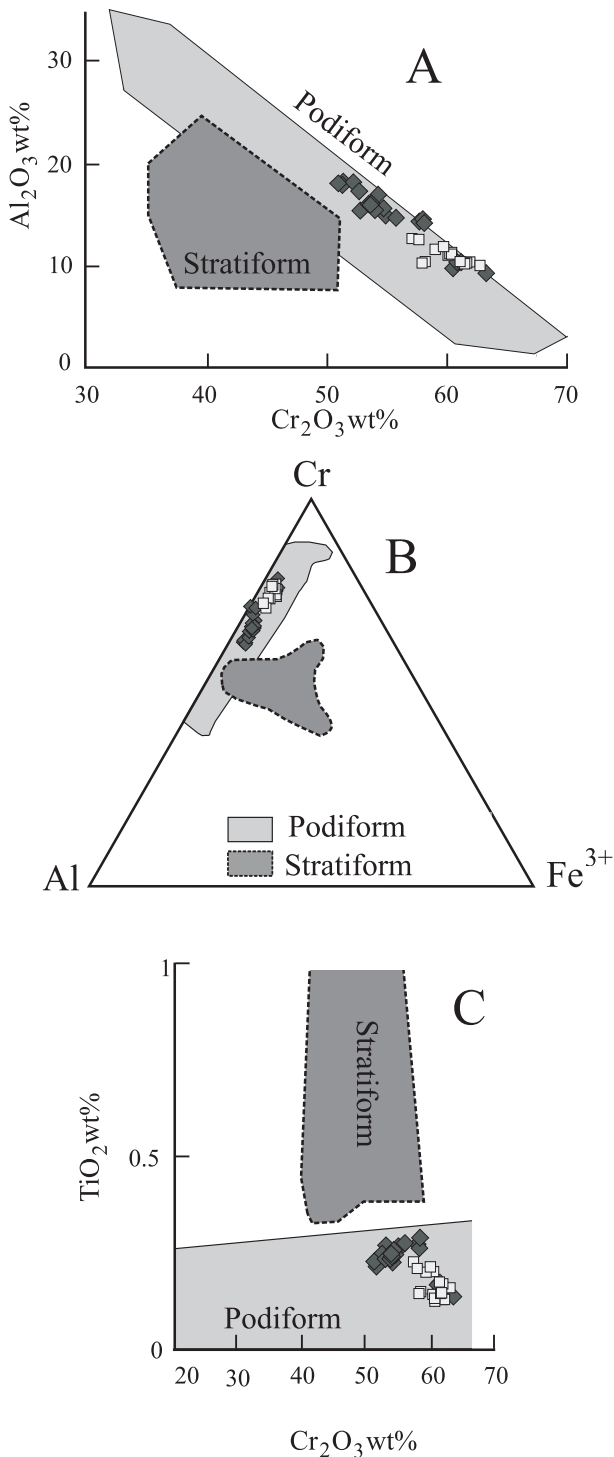


FIGURE 2 | Chemical composition of chromite, compared with stratiform and podiform chromitites on A) Cr_2O_3 wt% vs Al_2O_3 wt%, B) Cr–Al– Fe^{3+} B) and C) Cr_2O_3 wt% vs TiO_2 wt% diagrams. Podiform and stratiform fields are from Musallam et al. (1981) and Arai et al. (2004). Light squares: Kavak Mine and dark diamonds: Dağköplü Mine.

mation. Such inclusions may display a euhedral shape, but are usually anhedral or subhedral and are frequently associated with cracks or serpentine-filled veinlets in chromite. The latter group most probably formed or was re-mobilized during serpentinization.

Olivine, amphibole and rare clinopyroxene occur as inclusions, up to 100 μm in size, in the Dağköplü and Kavak chromite. Representative electron microprobe analyses are shown in Table 2 (see Appendix). Olivine is characterized by high Fo contents (i.e. Mg# = 95–98) and contains also high amounts of NiO (0.43–1.08 wt%) and Cr_2O_3 (up to 1.23 wt%). Clinopyroxenes have been classified as diopside and they have almost constant composition ($\text{En}_{49}\text{Fs}_2\text{Wo}_{49}$; Mg# = 96–97). They contain 0.28–0.39 wt% of Na_2O , 1.75–2.24 wt% of Cr_2O_3 and 0.50–0.72 wt% of Al_2O_3 . Amphiboles have been classified as tschermakite and hornblende. Amphiboles have generally high magnesium content (i.e. Mg# ranges from 94 to 98), and are enriched in Cr_2O_3 (2.81–4.68 wt%) and Na_2O (2.02–3.64 wt%). The contents of TiO_2 (0.18–0.46 wt%) and K_2O (up to 0.65 wt%) are very low. The analyses of silicate inclusions reveal that their Cr content is consistently high, independently of their size.

The following primary base-metal sulfide inclusions have been identified: millerite (NiS), godlevskite (Ni_7S_6), bornite (Cu_5FeS_4) and an unnamed Cu_2FeS_3 phase. Ni-arsenides such as maucherite ($\text{Ni}_{11}\text{As}_8$) and orcelite (Ni_5As_2) were also found in fresh chromite, unrelated to cracks and fissures of the chromite host. Therefore, they have been classified as primary inclusions. Heazlewoodite, awaruite, pyrite and rare putoranite ($\text{Cu}_9\text{Fe,Ni}_9\text{S}_{16}$) were detected in the matrix of chromite and considered as sec-

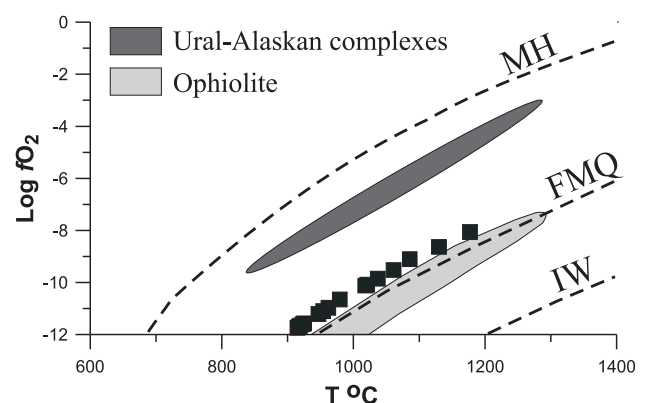


FIGURE 3 | Calculated temperature versus oxygen fugacity for Eskişehir chromitites. Data for the dark grey field of Ural-Alaskan-type complexes, and light grey field of dunite, harzburgite and chromitite from ophiolites of the Urals are from Chashchukin et al. (1998) and Pushkarev (2000). Lines for the MH, FMQ, and IW buffers with temperature are according to Ballhaus et al. (1991).

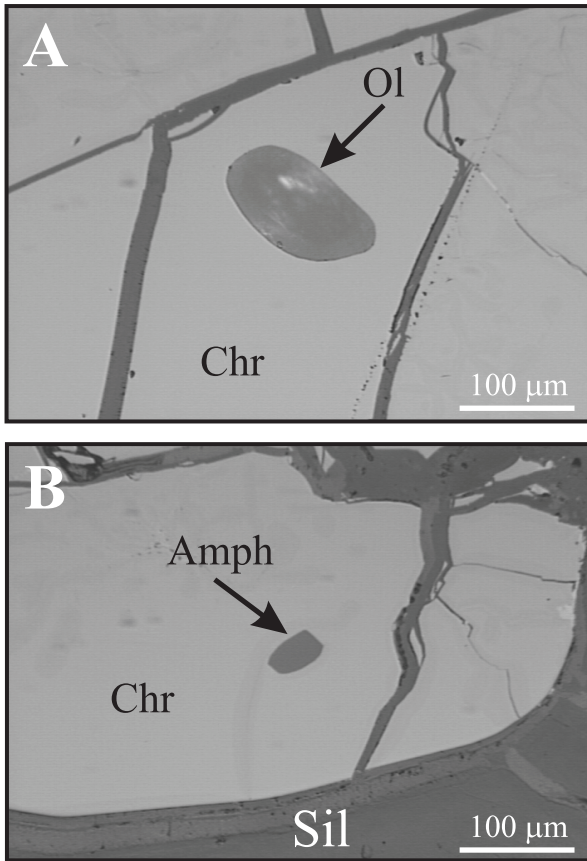


FIGURE 4 | Reflected light images of primary olivine and amphibole inclusions in chromite. Ol: Olivine, Amph: Amphibole, Chr: Chromite, Sil: Silicate.

ondary phases. Selected analyses of base-metal sulfides, arsenides and alloys are listed in Table 3 (see Appendix).

PGE GEOCHEMISTRY AND MINERALOGY

Total PGE concentrations in the analyzed chromitites vary between 109 and 533 ppb (Table 4, see Appendix). The chondrite-normalized PGE patterns of the chromitites, as illustrated in Fig. 5A, show a flat trend between Os and Ir, positive Ru anomaly, a negative slope between Ru and Pt, and a slight positive trend between Pt and Pd. The (Os+Ir+Ru)/(Rh+Pt+Pd) ratio in the Dağküplü and Kavak chromitites is quite variable, i.e. between 3.4 to 18. These values suggest an enrichment in the IPGE (i.e. Os, Ir, Ru) over the PPGE (i.e. Rh, Pt, Pd), as typical for mantle ophiolite-hosted chromitites. However, the ratio between Pd and Ir varies from 0.07 to 0.41 and is consistent with an unfractionated nature of the investigated chromitites (Barnes et al., 1985). PGE data plotted in the $PPGE_N / IPGE_N$ vs PGE and Pt/Pt* [= $Pt_N / (Rh_N * Pd_N)^{1/2}$] vs Pd/Ir diagrams proposed by Melcher et al. (1999) and Garuti et al. (1997) follow the ophiolitic trend (Fig. 5B) as well as a partial melting trend (Fig. 5C).

In accordance with the PGE concentrations (i.e. a positive Ru anomaly, Fig. 5A), the only PGM recognized in the Dağküplü and Kavak chromitites is laurite (ideally RuS_2). It occurs as euhedral to subhedral crystals, varying

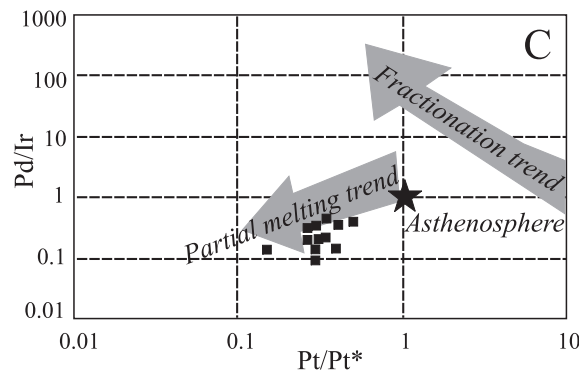
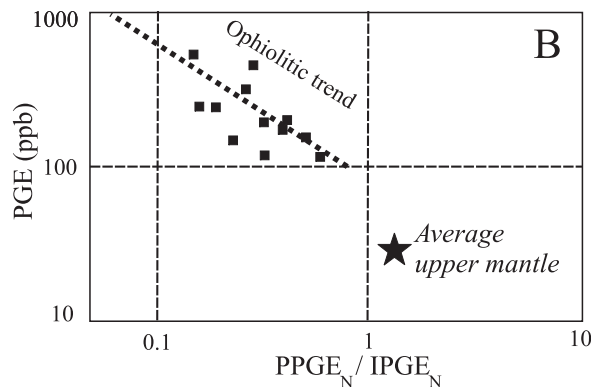
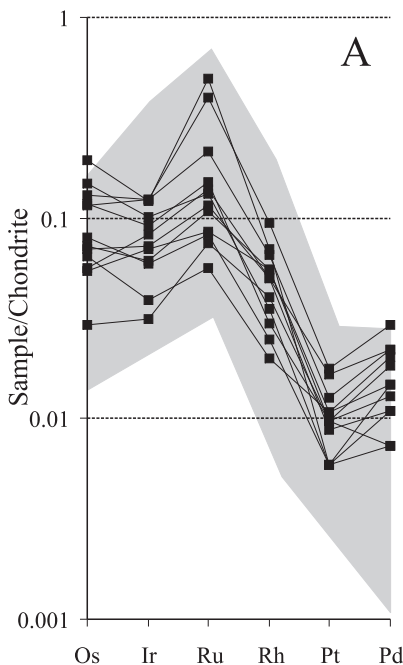


FIGURE 5 | A) Chondrite-C1 (Naldrett, 1981) normalized PGE patterns of the Eskişehir chromitites and comparison with the chromitites hosted in the ophiolitic mantle (grey field). Data from: Proenza et al. (1999); Economou-Eliopoulos (1996); McElduff and Stumpfl (1990); Gauthier et al. (1990); Kojonen et al. (2003); Büchl et al. (2004); Uysal et al. (2005); B) Chondrite-normalized $PPGE_N / IPGE_N$ vs PGE for the Eskişehir chromitites. Chondrite and average upper mantle values are from Leblanc (1991) and ophiolitic trend is from Melcher et al. (1999); C) Plot of $Pt/Pt^* [Pt_N / (Rh_N * Pd_N)^{1/2}]$ vs Pd/Ir of the Eskişehir chromitites. Fractionation and partial melting trends are from Garuti et al. (1997).

in size from 1 to 20 μm , always enclosed in fresh chromite. Laurite occurs both as monophase and composite grains, in association with amphibole, bornite and other base-metal sulfides (Fig. 6). Microprobe analyses of laurite revealed a compositional variation between $\text{Ru}_{0.94}\text{Os}_{0.03}\text{Ir}_{0.02}\text{S}_{1.95}$ and $\text{Ru}_{0.64}\text{Os}_{0.21}\text{Ir}_{0.10}\text{S}_{1.85}$ (Fig. 7, Table 5 in Appendix). It contains up to 1.96 at% of Rh and 3.67 at% of As.

DISCUSSION

The geotectonic environment and the formation of the Dağköplü and Kavak chromitites

The origin of mantle podiform chromitite deposits has been discussed for many years (Lago et al., 1982; Cassard et al., 1983; McElduff and Stumpfl, 1990; Arai, 1997; Zhou et al., 1998, Arai and Yurimoto, 1994; Ballhaus, 1998a,b; Melcher et al., 1997, 1999; Zhou et al., 1998, 2001 and references therein). Although many

genetic aspects are still not fully understood, there are basically three hypotheses concerning the genesis of podiform chromitites: i) podiform chromitites may represent part of the residuum after extensive extraction of melt from their mantle host, based on their association with the residual mantle rocks such as dunite and harzburgite, ii) podiform chromitites have been interpreted as a cumulate filling of a magma conduit inside the residual mantle, and iii) more recently, it has been stressed that such deposits form as a result of melt/rock or melt/melt interaction (i.e. “magma-mingling”). Furthermore, the presence of water in the melt is thought to be necessary for the crystallization of chromium spinel (Edwards et al., 2000). Experimental results from water-oversaturated basalts by Matveev and Ballhaus (2002) suggest that podiform chromitites form from primitive water-enriched melts saturated in olivine-chromite.

The Dağköplü and Kavak chromitites clearly represent typical podiform chromitites. They contain abundant primary olivine inclusions, characterized by very high fo-contents (i.e. Mg# from 95 to 98), indicating that the chromite crystallized from a primitive olivine-chromite saturated melt at magmatic temperatures. Experimental work demonstrated that high amounts of Cr and Ni can be incorporated in the olivine lattice only at high temperatures of around 1200°C (Lehmann, 1983; Li et al., 1995). The rare Cr-rich clinopyroxene inclusions might indicate that the Si-activity was rather high in the melt at the time of chromium spinel crystallization. The chromite composition with respect to high Cr-concentrations, distinct to Al-rich chromites, as well as the TiO_2 and Al_2O_3 concentrations (Fig. 8A, B) show a good match with chromitites crystallized from a

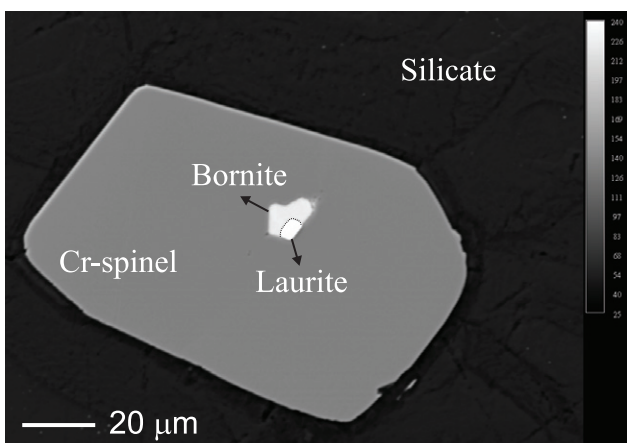
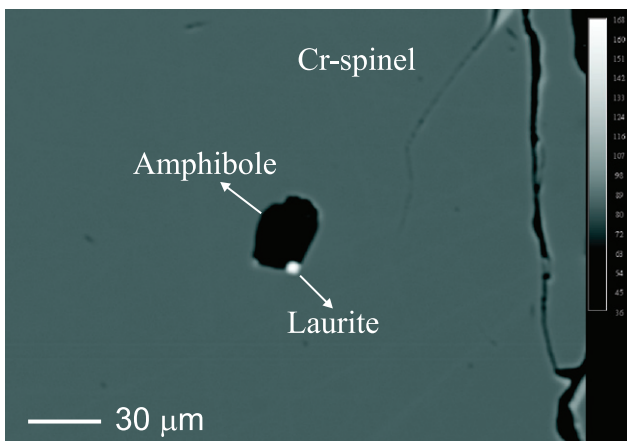


FIGURE 6 | Back scattered electron (BSE) images of laurite grains coexisting with A) hydrous silicate of amphibole and B) bornite.

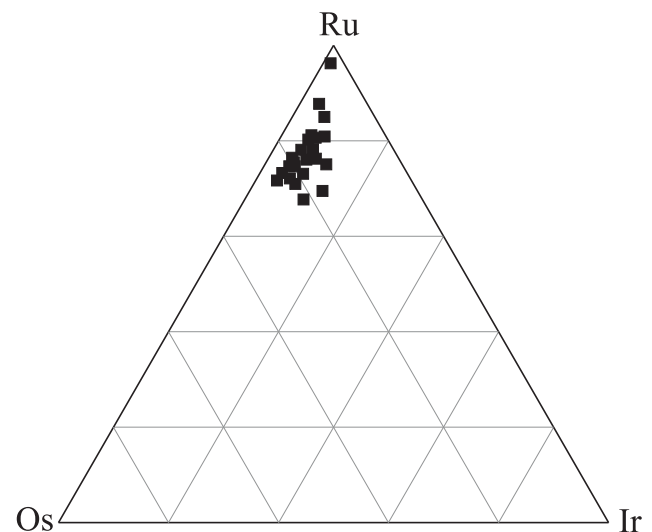


FIGURE 7 | Composition of laurite inclusions (at%) in chromite of Eskişehir chromitites plotted on the Ru-Os-Ir triangle.

boninitic melt, formed in a suprasubduction zone (SSZ) environment and is distinct from that related to middle oceanic ridge basalts (MORB) (Kamenetsky et al., 2001). Therefore, we suggest that the Dağküplü and Kavak chromitites have crystallized from a boninite melt within a SSZ setting.

Moreover, the chromium spinels of the Dağküplü and Kavak chromitites contain abundant Cr-Na-rich amphibole inclusions. They are considered as primary inclusions, implying that they have been included contemporaneously with chromite crystallization at high magmatic temperatures, or later during annealing and sintering processes related with post-magmatic hydrothermal activities. In either way amphibole inclusions are considered as a good indication for the presence of a fluid phase during chromite precipitation. Experimental results showed that pargasitic amphibole associated with chromite may crystallize at temperatures between 950° to 1050°C at oxygen fugacity varying between that of the FeO/Fe and NiO/Ni buffers (Wallace and Green, 1991). These temperatures lie within the range of chromium spinel crystallization temperatures of the Dağküplü and Kavak chromitites obtained by chromite-olivine geothermometry.

The presence of primary inclusions of millerite, godlevskite, bornite, and Cu_2FeS_3 phases in chromite crystals indicate the increasing sulfur fugacity conditions during the chromite crystallization. Close association of bornite and laurite, completely included in fresh chromite as shown in Figure 6B, support their magmatic origin. The inclusions of base-metal arsenides of maucherite and orcelite were trapped in chromite probably at lower temperature, later than base-metal sulfides and laurites, and are clear indicative of high As activity at the time of chromite crystallization.

The PGE in the chromitites from Dağküplü and Kavak

The chondrite-normalised PGE distribution patterns (Fig. 5A) from Dağküplü and Kavak are typical for podiform chromitites. In accordance with the predominance of IPGE, laurite was the only PGM identified as inclusion in chromite. The shape of laurite, its textural relationship to the chromite host and association with sulfides, and its chemical composition clearly indicate that laurite was part of the chromite precipitation. The lack of any IPGE alloys, as well as the low Os-content of laurite, assumes that laurite was crystallizing at increasing $f\text{S}_2$ conditions of the magma.

The total PGE concentration in the Dağküplü and Kavak chromitites is low (i.e. between 109 and 533

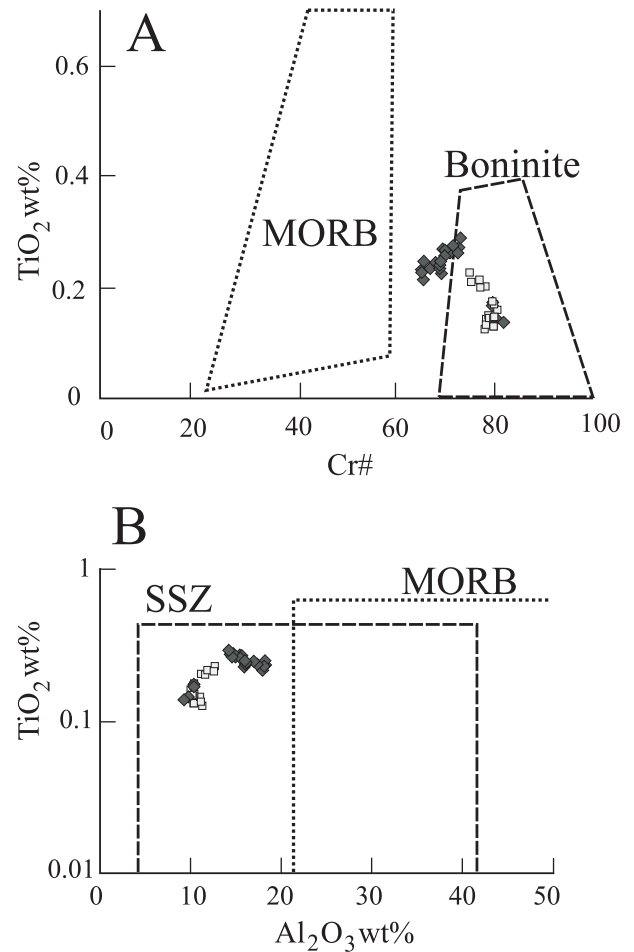


FIGURE 8 | Composition of chromite of Eskişehir chromitites on A) Cr# vs TiO₂ wt% and B) Al₂O₃ wt% vs TiO₂ wt% diagrams. Fields of MORB (Mid-ocean ridge basalts) and boninite in Figure 3A are from Dick and Bullen (1984) and Arai (1992) and fields of MORB and SSZ (Suprasubduction zone) are from Kamenetsky et al. (2001). Light squares: Kavak Mine and dark diamond: Dağküplü Mine.

ppb), thus not of economic importance at present. However, the PGE show a growing use in advanced technologies, such as electronics, medical and auto catalysts, and are thus considered as strategic metals. Furthermore, there is an increasing demand, and a steady increase of PGE prices on the international market. These circumstances justify continuous exploration on PGE in the Dağküplü and Kavak chromitites.

SUMMARY AND CONCLUSIONS

This paper presents the first detailed investigation on the chromitites of the Dağküplü and Kavak mines, located in the Eskişehir ophiolite (N-W Turkey). The results, based on the chromite composition and asso-

ciated primary inclusions, indicate i) chromite precipitation from a boninite magma in a SSZ environment, in agreement with the geodynamic setting proposed for the Eskişehir ophiolite (Sarifikioğlu, 2007), ii) chromite crystallization starting at temperatures of around 1290°C, iii) abundant Na-rich amphibole inclusions clearly indicate the presence of a sodium-rich fluid phase during the crystallization of the chromium spinel, iv) the PGE concentration is characterized by IPGE dominance, typical for ophiolite deposits, v) the lack of Os-Ir alloys and erlichmanite in the PGM paragenesis, and presence of laurite with low Os content reveal that laurite crystallized at relatively high (fS_2) below the Os-OsS₂ buffer.

The small size of laurite (i.e. less than 15 µm in diameter) and the low total PGE concentrations preclude the Dağköplü and Kavak chromitites to represent a potential target for PGE recovery at present.

ACKNOWLEDGEMENTS

This study was financially supported by Karadeniz Technical University through a Socrates/Erasmus and DAAD (German Academic Exchange Services) scholarships to I. Uysal. We express our sincere thanks to P. Stutz for his help in the laboratory and for preparing polished sections. We are very grateful to S. Heidrich for her assistance and great patience during the electron-microprobe analyses. A.H. Aygün is thanked for his never ending help during the field trip and sample collections. We thank Lorena Ortega and Evgeny Pushkarev who provided constructive reviews and Joaquin Proenza for his careful handling of the manuscript.

REFERENCES

- Ahmed, A.H., Arai, S., 2002. Unexpectedly high PGE chromitite from the deeper mantle section of the northern Oman ophiolite and its tectonic implications. *Contribution to Mineralogy and Petrology*, 143, 263-278.
- Arai, S., 1992. Chemistry of chromian spinel in volcanic rocks as a potential guide to magma chemistry. *Mineralogical Magazine*, 56, 173-184.
- Arai, S., 1997. Origin of podiform chromitites. *Journal of Asian Earth Sciences*, 15, 303-310.
- Arai, S., Yurimoto, H., 1994. Podiform chromitites of the Tami-Misaka ultramafic complex, Southwestern Japan, as mantle-melt interaction products. *Economic Geology*, 89, 1279-1288.
- Arai, S., Uesugi, J., Ahmed, A.H., 2004. Upper Crustal Podiform Chromitite From The Northern Oman Ophiolite as The Stratigraphically Shallowest Chromitite in Ophiolite and Its Implication for Cr Concentration. *Contribution to Mineralogy and Petrology*, 147, 145-154.
- Ballhaus, C., 1998a. Origin of podiform chromite deposits. *Geological Society of South Africa*, 18, 21-24.
- Ballhaus, C., 1998b. Origin of podiform chromite deposits by magma mingling. *Earth Planetary Science Letters*, 156, 185-193.
- Ballhaus, C., Berry, R.F., Green, D.H., 1991. High pressure experimental calibration on the olivine-orthopyroxene-spinel oxygen geobarometer: implications for the oxidation state of the upper mantle. *Contributions to Mineralogy and Petrology*, 107, 27-40.
- Barnes, S.J., Naldrett, A.J., Gorton, M.P., 1985. The origin of the fractionation of platinum group elements in terrestrial magmas. *Chemical Geology*, 53, 303-323.
- Beklioglu, B., Arol, A.I., 2004. Selective flocculation behavior of chromite and serpentine. *Physicochemic. Problems Mineral Processes*, 38, 10-112.
- Büchl, A., Brugmann, G., Batanova, V.G., 2004. Formation of Podiform Chromitite Deposits, Implication From PGE Abundances and Os Isotopic Composition of Chromites From the Troodos Complex, Cyprus. *Chemical Geology*, 208, 217-232.
- Cassard, D., Nicolas, A., Rabinowicz, M., Moutte, J., Leblanc, M., Prinzhofer, A., 1983. Structural classification of chromite pods in southern New Caledonia. *Economic Geology*, 76, 805-831.
- Chashchukin, I.S., Votyakov, S.L., Uimin, S.G., 1998. Oxygen thermometry and barometry in chromite-bearing ultramafic rocks: an example of ultramafic massifs on the Urals. II. Oxidation state of ultramafics and the composition of mineralizing fluids. *Geochemistry International*, 36, 783-791.
- Dick, H.J.B., Bullen, T., 1984. Chromian spinel as a petrogenetic indicator in abyssal and alpine-type peridotites and spatially associated lavas. *Contributions to Mineralogy and Petrology*, 86, 54-76.
- Distler, V.V., Kryachko, V.V., Yudovskaya, M.A., 2008. Ore petrology of chromite-PGE mineralization in the Kempirsai ophiolite complex. *Mineralogy and Petrology*, 92, 31-58.
- Economou-Eliopoulos, M., 1993. Platinum-group elements (PGE) distribution in chromite ores from ophiolite complexes of Greece: implications for chromite exploration. *Ophiolite*, 18, 83-97.
- Economou-Eliopoulos, M., 1996. Platinum-group elements distribution in chromite ores from ophiolite complexes: implications for their exploration. *Ore Geology Review*, 11, 363-381.
- Economou-Eliopoulos, M., Vacondios, M., 1995. Geochemistry of the chromitites and host rocks from the Pindos ophiolite complex, northwestern Greece. *Chemical Geology*, 122, 99-108.
- Edwards, S.J., Pearce, J.A., Freeman, J., 2000. New insights concerning the influence of water during the formation of podiform chromite. In: Dilek, Y., Moores, E.M., Elthon, D., Nicolas, A. (eds.). *Ophiolites and oceanic crust: new insights from field studies and the ocean drilling program: Boulder, Colorado. Geological Society of America Special Paper*, 349, 139-147.
- Eskikaya, S., Aydinler, S., 2000. Expectation and realization-full achievement of the objectives in terms of profitability and safety in Kavak chrome mine. Las Vegas, presentation at Mine Expo 2000, 17.
- Garuti, G., Fershtater, G., Bea, F., Montero, P.G., Pushkarev, E.V., Zaccarini, F., 1997. Platinum-group element distribution in mafic-ultramafic complexes of central and southern Urals: Preliminary results. *Tectonophysics*, 276, 181-194.

- Garuti, G., Zaccarini, F., Economou-Eliopoulos, M., 1999. Paragenesis and composition of laurite from chromitites of Othrys (Greece): implications for Os-Ru fractionation in ophiolitic upper mantle of the Balkan Peninsula. *Mineralium Deposita*, 34, 312-319.
- Gauthier, M., Corrivaux, L., Trottier, L.J., Cabri, L.J., Laflamme, J.H.G., Bergeron, M., 1990. Chromitites Platinifères de l'Estrie-Beauce, Appalaches du sud de Québec. *Mineralium Deposita*, 25, 169-178.
- Kamenetsky, V.S., Crawford, A.J., Meffre, S., 2001. Factors controlling chemistry of magmatic spinel: an empirical study of associated olivine, Cr-spinel and melt inclusions from primitive rocks. *Journal of Petrology*, 42, 655-671.
- Kocks, H., Melcher, F., Meisel, T., Burgath, K.P., 2007. Diverse contributing sources to chromitite petrogenesis in the Shebenik Ophiolitic Complex, Albania: evidence from new PGE and Os-isotope data. *Mineralogy and Petrology*, 91, 139-170.
- Kojonen, K., Zaccarini, F., Garuti, G., 2003. Platinum-Group Elements and Gold Geochemistry and Mineralogy in the Ray-Iz Ophiolitic Chromitites, Polar Urals. In: Eliopoulos, D.G. et al. (eds.). *Mineral Exploration and Sustainable Development*, Millpress Rotterdam Netherlands, 599-602.
- Kostantopoulou, G., Economou-Eliopoulos, M., 1991. Distribution of platinum-group elements and gold within the Vourinos chromitite ores, Greece. *Economic Geology*, 86, 1672-1682.
- Lago, B.L., Rabinowicz, M., Nicolas, A., 1982. Podiform chromite ore bodies: a genetic model. *Journal of Petrology*, 23, 103-125.
- Leblanc, M., 1991. Platinum-group Elements and Gold in Ophiolitic Complexes, Distribution and Fractionation from Mantle to Oceanic Floor. In: Peters, T. et al. (eds.). *Ophiolite Genesis and Evolution of The Oceanic Lithosphere*, Oman, Kluwer, Dordrecht, 231-260.
- Lehmann, J., 1983. Diffusion between olivine and spinel: application to geothermometry. *Earth and Planetary Science Letter*, 64, 123-138.
- Li, J.-P., O'Neill, H. St. C., Seifert, F., 1995. Subsolidus phase relations in the system MgO-SiO₂-Cr-O in equilibrium with metallic Cr, and their significance for the petrochemistry of chromium. *Journal of Petrology*, 36, 107-132.
- Malitch, K.N., Thalhammer, O.A.R., Knauf, V.V., Melcher, F., 2003. Diversity of platinum group mineral assemblages in banded and podiform chromitite from the Kraubath ultramafic massif, Austria: evidence for an ophiolitic transition zone? *Mineralium Deposita*, 38, 282-297.
- Matveev, S., Ballhaus, C., 2002. Role of water in the origin of podiform chromitite deposits. *Earth and Planetary Science Letters*, 203, 235-243.
- McEllduff, B., Stumpfl, E.F., 1990. The chromite deposits of the Troodos complex, Cyprus - Evidence for the role of a fluid phase accompanying chromite formation. *Mineralium Deposita*, 26, 307-318.
- Melcher, F., Grum, W., Simon, G., Thalhammer, T.V., Stumpfl, E.F., 1997. Petrogenesis of the ophiolitic giant chromite deposits of Kempirsai, Kazakhstan: a study of solid and fluid inclusions in chromite. *Journal of Petrology*, 38, 1419-1458.
- Melcher, F., Grum, W., Thalhammer, T.V., Thalhammer, O.A.R., 1999. The giant chromite deposits at Kempirsai, Urals: constraints from trace element (PGE, REE) and isotope data. *Mineralium Deposita*, 34, 250-272.
- Mussallam, K., Jung, D., Burgath, K., 1981. Textural features and chemical characteristics of chromites in ultramafic rocks, Chalkidiki complex (Northeastern Greece), TMPM Tschermarks *Mineralogische und Petrographische Mitteilungen.*, 29, 75-101.
- Naldrett, A.J., 1981. Platinum-Group Element Deposits. In: Cabri, L.J. (eds.). *PGE Mineralogy, Geology, Recovery*. Canadian Institute of Mineralogy and Metallogeny, 23, 197-231.
- Okay, A.I., 1984. Distribution and characteristics of the northwest Turkish blueschists. In: Dixon, J.E. and Robertson, A.H.F. (eds.), *The Geological Evolution of the Eastern Mediterranean*. Geological Society of London, Special Publication, 17, 455-466.
- Proenza, J.A., Gervilla, F., Melgarejo, J.C., Bodinier, J.L., 1999. Al and Cr rich chromitites from the Mayari-Baracoa Ophiolitic Belt, (eastern Cuba): consequence of interaction between volatile-rich melts and peridotite in suprasubduction mantle. *Economic Geology*, 94, 547-566.
- Proenza, J.A., Zaccarini, F., Escayola, M., Cábana, C., Schalamuk, A., Garuti, G., 2008. Composition and textures of chromite and platinum-group Minerals in chromitites of the western ophiolitic belt from Pampean Ranges of Córdoba, Argentina. *Ore Geology Reviews*, 33, 32-48.
- Pushkarev, E.V., 2000. Petrology of the Uktus dunite-clinopyroxenite-gabbro massif (the Middle Urals). Ekaterinburg, Institute of Geology and Geochemistry Ural Branch, RAS, 296 pp. (in Russian).
- Rechenberg, H.P., 1960. The chrome ore deposit of Kavak, Eskişehir, Turkey. Ankara, Symposium on chrome-ore-CEN-TO, 146-156.
- Sarifakioglu, E., 2007. Petrology and origin of plagiogranites from the Dağköplü (Eskişehir) ophiolite along the Izmir-Ankara-Erzincan suture zone, Turkey. *Ofioliti*, 32, 39-51.
- Şengör, A.M.C., 1987. Tectonics of the Tethysides: Orogenic collage development in a collisional setting. *Annual Review of Earth and Planetary Science*, 15, 213-244.
- Thalhammer, O.A.R., Prochaska, W., Mühlans, H.W., 1990. Solid inclusion in chrome-spinels and platinum-group element concentration from the Hochgrößen and Kraubath ultramafic massifs (Austria). *Contributions to Mineralogy and Petrology* 105, 66-80.
- Uysal, I., Sadiklar, M.B., Tarkian, M., Karsli, O., Aydin, F., 2005. Mineralogy and composition of the chromitites and their platinum-group minerals from Ortaca (Muğla-SW Turkey): evidence for ophiolitic chromitite genesis. *Mineralogy and Petrology*, 83, 219-242.
- Uysal, I., Tarkian, M., Sadiklar, M.B., Şen, C., 2007a. Platinum-group-elements geochemistry and mineralogy in ophiolitic chromitites from the Kop Mountains, northeastern Turkey. *The Canadian Mineralogist*, 45, 355-377.

- Uysal, I., Zaccarini, F., Garuti, G., Meisel, T., Tarkian, M., Bernhardt, H.J., Sadiklar, M.B., 2007b. Ophiolitic chromitites from the Kahramanmaraş area, southeastern Turkey: Their platinum-group elements (PGE) geochemistry, mineralogy and Os-isotope signature. *Ophioliti*, 32, 151-161.
- Wallace, M.E., Green, D.H., 1991. The effect of bulk composition on the stability of amphibole in the upper mantle: implications for solidus positions and mantle metasomatism. *Mineralogy and Petrology*, 44, 1-19.
- Zaccarini, F., Pushkarev, E., Garuti, G., 2008. Platinum-group element mineralogy and geochemistry of chromitite of the Kluchevskoy ophiolite complex, central Urals (Russia). *Ore Geology Reviews*, 33, 20-30.
- Zhou, M.F., Sun, M., Keays, R.R., Kerrich, R., 1998. Controls on platinum-group elemental distributions of podiform chromitites: a case study of high-Cr and high-Al chromitites from Chinese orogenic belts. *Geochimica, Cosmochimica Acta*, 62, 677-688.
- Zhou, M.F., Robinson, P.T., Malpas, J., Aitchison, J., Sun, M., Bai, W.J., Hu, X.F., Yang, J.S., 2001. Melt/mantle interaction and melts evolution in the Sartohay high-Al chromite deposits of the Salabute ophiolite (NW China). *Journal of Asian Earth Sciences*, 19, 517-534.

Manuscript received February 2008;
revision accepted August 2008;
published Online April 2009.

APPENDIX

Analytical data

TABLE 1 | Selected electron microprobe composition (wt%) and atomic proportions of chromite of Dağküpü and Kavak chromitites from the Eskişehir. $Mg\# = Mg/(Mg+Fe^{2+})$, $Cr\# = Cr/(Cr+Al)$, $Fe^{3+\#} = Fe^{3+}/(Cr+Al+Fe^{3+})$.

wt%	Dağküpü									Kavak					
	Es9-1	Es9-2	Es5-1	Es7-2	Es11-1	Es3B-2	Es12-1	Es2B-1	Es10-1	EkMO-4	EkMO-2	Ek4-1	Ek4-2	EkMO-1	Ek2
TiO ₂	0.23	0.27	0.23	0.23	0.14	0.28	0.25	0.29	0.17	0.13	0.14	0.13	0.16	0.15	0.23
Al ₂ O ₃	16.07	15.42	15.92	18.11	9.74	14.72	15.99	14.21	10.37	10.33	11.05	11.30	10.02	10.28	12.68
Cr ₂ O ₃	53.53	52.85	53.89	51.02	60.53	55.79	53.68	58.15	61.20	61.61	60.12	60.43	62.77	57.97	57.12
Fe ₂ O ₃	3.15	3.07	2.41	3.30	3.11	1.46	2.68	1.18	3.21	2.94	2.83	2.73	2.41	3.44	3.12
FeO	13.55	13.57	12.86	12.72	12.30	13.66	13.54	13.95	13.13	11.46	12.87	13.91	10.97	12.32	16.08
MnO	0.15	0.17	0.09	0.13	0.17	0.11	0.15	0.20	0.19	0.07	0.14	0.07	0.00	0.16	0.21
NiO	0.07	0.08	0.08	0.14	0.07	0.14	0.12	0.07	0.12	0.24	0.13	0.19	0.10	0.03	0.08
MgO	13.85	13.40	14.09	14.47	13.80	13.46	13.73	13.64	13.77	14.70	13.79	13.35	15.16	13.43	11.99
CaO	0.00	0.00	0.03	0.00	0.00	0.00	0.00	0.02	0.01	0.00	0.01	0.01	0.02	0.00	0.01
Total	100.60	98.83	99.60	100.12	99.86	99.62	100.14	101.71	102.17	101.48	101.08	102.12	101.61	97.78	101.52
At. prop.															
Ti	0.006	0.006	0.005	0.005	0.003	0.007	0.006	0.007	0.004	0.003	0.003	0.003	0.004	0.004	0.005
Al	0.592	0.580	0.591	0.662	0.371	0.551	0.592	0.523	0.386	0.385	0.414	0.420	0.372	0.399	0.476
Cr	1.323	1.334	1.342	1.251	1.547	1.401	1.333	1.435	1.530	1.539	1.512	1.509	1.562	1.509	1.439
Fe ³⁺	0.074	0.074	0.057	0.077	0.076	0.035	0.063	0.028	0.076	0.070	0.068	0.065	0.057	0.085	0.075
Fe ²⁺	0.354	0.362	0.339	0.330	0.332	0.363	0.356	0.364	0.347	0.303	0.342	0.367	0.289	0.339	0.428
Mn	0.004	0.005	0.002	0.003	0.005	0.003	0.004	0.005	0.005	0.002	0.004	0.002	0.000	0.004	0.006
Ni	0.002	0.002	0.002	0.003	0.002	0.004	0.003	0.002	0.003	0.006	0.003	0.005	0.003	0.001	0.002
Mg	0.645	0.637	0.661	0.669	0.664	0.637	0.643	0.635	0.649	0.692	0.654	0.629	0.712	0.659	0.569
Ca	0.000	0.000	0.001	0.000	0.000	0.000	0.000	0.001	0.000	0.000	0.000	0.000	0.001	0.000	0.000
Total	3.000	3.000	3.000	3.000	3.000	3.000	3.000	3.000	3.000	3.000	3.000	3.000	3.000	3.000	3.000
Mg#	64.6	63.8	66.1	67.0	66.7	63.7	64.4	63.5	65.1	69.6	65.6	63.1	71.1	66.0	57.1
Cr#	69.1	69.7	69.4	65.4	80.7	71.8	69.3	73.3	79.8	80.0	78.5	78.2	80.8	79.1	75.1
Fe ³⁺ #	3.7	3.7	2.9	3.9	3.8	1.8	3.2	1.4	3.8	3.5	3.4	3.3	2.9	4.3	3.8

TABLE 2 | Selected electron microprobe composition (wt%) and atomic proportions of primary silicate inclusions in chromite of Eskişehir chromitites. Total iron is expressed as FeO.

wt%	Ek2-5	EkMO4-3	EkMO4-5	Ek4-2-4	Ek4-2-14	EkMO4-6	EkMO4-7	EkMO1-9	EkMO2-4	EkMO2-9	Ek4-2-12	EkMO1-6	Ek3-3-5
	Olivine					Clinopyroxene			Amphibole				
SiO ₂	41.41	41.47	41.63	41.67	41.81	53.25	53.36	53.72	44.53	44.08	44.39	43.96	48.07
TiO ₂	0.02	0.00	0.03	0.00	0.00	0.03	0.05	0.02	0.33	0.32	0.37	0.20	0.46
Al ₂ O ₃	0.01	0.01	0.01	0.00	0.01	0.63	0.50	0.72	10.53	11.11	11.16	11.06	7.54
Cr ₂ O ₃	0.67	0.85	0.44	0.54	0.81	2.24	2.16	1.75	3.57	4.00	4.20	3.91	3.23
FeO	4.33	2.29	2.81	2.33	2.28	1.07	1.01	1.21	1.63	1.55	1.57	1.83	1.40
MnO	0.05	0.01	0.03	0.06	0.05	0.00	0.00	0.01	0.00	0.04	0.00	0.00	0.02
NiO	0.55	0.91	0.85	0.97	0.97	0.03	0.05	0.10	-	-	-	-	-
MgO	54.02	55.40	54.81	55.27	55.19	18.04	18.06	17.90	20.43	20.32	20.38	20.51	22.06
CaO	0.02	0.02	0.01	0.02	0.03	24.82	24.79	24.64	12.64	12.84	11.86	12.76	12.45
Na ₂ O	0.01	0.00	0.00	0.02	0.00	0.28	0.27	0.40	3.25	3.28	3.56	3.58	2.02
K ₂ O	0.00	0.00	0.00	0.00	0.00	0.00	0.01	0.01	0.03	0.09	0.08	0.07	0.10
Total	101.09	100.96	100.62	100.88	101.15	100.39	100.26	100.48	96.94	97.63	97.57	97.88	97.35
At. prop.													
O	4	4	4	4	4	6	6	6	23	23	23	23	23
Si	0.984	0.980	0.988	0.985	0.986	1.937	1.942	1.949	6.337	6.248	6.279	6.224	6.740
Ti	0.000	0.000	0.000	0.000	0.000	0.001	0.001	0.000	0.036	0.034	0.039	0.022	0.049
Al	0.000	0.000	0.000	0.000	0.000	0.027	0.021	0.031	1.767	1.856	1.861	1.845	1.247
Cr	0.013	0.016	0.008	0.010	0.015	0.064	0.062	0.050	0.401	0.448	0.470	0.437	0.358
Fe	0.086	0.045	0.056	0.046	0.045	0.033	0.031	0.037	0.194	0.183	0.186	0.216	0.164
Mn	0.001	0.000	0.001	0.001	0.001	0.000	0.000	0.000	0.000	0.005	0.000	0.000	0.002
Ni	0.010	0.017	0.016	0.018	0.018	0.001	0.001	0.003	-	-	-	-	-
Mg	1.914	1.952	1.938	1.948	1.940	0.978	0.980	0.968	4.334	4.294	4.298	4.328	4.611
Ca	0.000	0.001	0.000	0.001	0.001	0.967	0.967	0.958	1.927	1.949	1.797	1.935	1.871
Na	0.000	0.000	0.000	0.001	0.000	0.020	0.019	0.028	0.897	0.902	0.977	0.983	0.548
K	0.000	0.000	0.000	0.000	0.000	0.000	0.000	0.000	0.005	0.016	0.015	0.012	0.017
Total	3.008	3.011	3.007	3.010	3.006	4.028	4.024	4.024	15.898	15.935	15.922	16.002	15.607
Mg#	95.7	97.7	97.2	97.7	97.7	96.8	97.0	96.4	95.7	95.9	95.9	95.2	96.6

TABLE 3 | Selected electron microprobe composition (wt%) and atomic proportions of primary and secondary base-metal minerals (BMM) in the Eskişehir chromitites. Bor: Bornite, God: Godlevskite, Mil: Millerite, Mau: Maucherite, Orc: Orceite, Heaz: Heazlewoodite, Awa: Awaruite, Put: Putoranite, Pyr: Pyrite.

wt%	Es10	Es12	Ek2-3	Ek4-2	EkMO	Ek4-3	Ek4-4	Ek4-5	Ek4-6	EkMO2	Es11	EkMO1	Ek2-1	Ek4-1	Ek2-2
	Bor	God	Mil	Mau	Orc	Heaz	Awa	Put	Pyr						
Ni	0.02	0.03	62.53	59.36	49.57	63.85	67.84	68.69	69.61	72.05	73.03	73.36	1.83	2.79	13.47
Fe	10.90	6.75	3.17	1.34	0.55	0.15	1.01	0.79	0.62	0.16	23.35	23.37	28.90	42.39	32.20
Cu	59.99	68.16	0.00	0.00	0.00	0.00	0.00	0.00	0.00	0.00	0.24	0.56	32.53	0.00	0.02
Co	0.00	0.00	0.00	0.00	0.08	0.00	0.00	0.00	0.11	0.00	0.00	0.00	0.00	0.00	0.00
Cr	2.94	1.90	2.20	3.14	1.76	0.53	3.86	2.46	2.65	0.10	2.05	0.28	0.36	0.73	0.78
S	25.18	23.27	32.95	35.07	0.00	0.06	26.56	26.64	26.86	26.94	0.02	0.02	35.09	53.07	52.75
As	0.01	0.00	0.00	0.07	50.31	35.61	0.32	0.10	0.06	0.03	0.38	0.07	0.07	0.05	0.03
Total	99.04	100.11	100.85	98.98	102.27	100.20	99.59	98.68	99.91	99.28	99.07	97.66	98.78	99.03	99.25
At. prop.															
Ni	0.001	0.002	8.262	0.924	10.279	4.633	2.777	2.836	2.840	2.961	0.728	0.743	0.062	0.058	0.279
Fe	0.985	0.618	0.440	0.022	0.120	0.011	0.043	0.034	0.026	0.007	0.244	0.248	1.028	0.919	0.702
Cu	4.764	5.483	0.000	0.000	0.000	0.000	0.000	0.000	0.000	0.000	0.002	0.005	1.018	0.000	0.000
Co	0.000	0.000	0.000	0.000	0.015	0.000	0.000	0.000	0.005	0.000	0.000	0.000	0.000	0.000	0.000
Cr	0.286	0.187	0.329	0.055	0.413	0.043	0.179	0.114	0.122	0.005	0.023	0.003	0.014	0.017	0.018
Metal	6.036	6.290	9.031	1.001	10.827	4.687	2.999	2.984	2.993	2.973	0.997	0.999	2.122	0.994	0.999
S	3.963	3.710	7.969	0.998	0.000	0.009	1.991	2.013	2.005	2.026	0.000	0.000	2.176	2.005	2.001
As	0.001	0.000	0.000	0.001	8.173	2.024	0.010	0.003	0.002	0.001	0.003	0.001	0.002	0.001	0.001
Anion	3.964	3.710	7.969	0.999	8.173	2.033	2.001	2.016	2.007	2.027	0.003	0.001	2.178	2.006	2.001
Total	10.000	10.000	17.000	2.000	19.000	6.720	5.000	5.000	5.000	5.000	1.000	1.000	4.300	3.000	3.000

TABLE 4 | **Platinum-Group Element (PGE) concentrations (ppb) and calculated values for the Eskişehir chromitites. $Pt/Pt^* = Pt_N/(Rh_N + Pd_N)^{1/2}$.**

	Os	Ir	Ru	Rh	Pt	Pd	Σ PGE	Pd/Ir	PPGE _N / IPGE _N	Pt/Pt*
Ek4	59	67	275	19	18	16	454	0.24	0.29	0.27
EkMO4	15	17	52	8	10	7	109	0.41	0.60	0.35
Ek2	29	45	96	10	9	6	195	0.13	0.33	0.31
Ek3	37	33	74	11	10	4	169	0.12	0.40	0.40
Ek3-3	100	66	339	14	6	8	533	0.12	0.16	0.15
EkMO2	77	55	91	7	6	4	240	0.07	0.17	0.30
Es2	41	32	57	5	6	6	147	0.19	0.24	0.29
Es7	67	67	148	13	13	12	320	0.18	0.27	0.28
Es8	36	39	80	10	17	12	194	0.31	0.43	0.41
Es12	28	38	59	11	11	11	158	0.29	0.52	0.26
Es3	33	21	39	4	11	8	116	0.38	0.33	0.51
Es6	60	49	105	6	10	10	240	0.20	0.20	0.34

TABLE 5 | **Selected electron microprobe composition (wt%) and atomic proportions of primary laurite inclusions in chromite of the Eskişehir chromitites.**

wt%	Es5-1-3	Es7-1-1	Es7-1-2	Es7-2-1	Es5-2-2	Es2B-1-2	Ek4-1-5	Ek3-3-7	Ek3-3-7	Es10-1-2	Es10-1-3
Os	20.04	19.49	15.93	15.45	24.29	9.07	16.76	13.66	14.67	2.50	19.96
Ir	9.64	4.23	12.89	7.87	3.60	6.73	7.07	10.96	6.80	1.73	4.55
Ru	33.08	41.03	34.81	40.05	37.43	46.56	39.80	38.80	41.13	54.33	38.63
Rh	3.09	0.31	0.91	0.78	0.42	1.23	0.87	1.42	2.45	3.17	1.57
Pt	0.00	0.00	0.00	0.00	0.00	0.00	0.00	0.00	0.00	0.00	0.00
Pd	0.25	0.02	0.10	0.10	0.00	0.05	0.02	0.06	0.00	0.24	0.18
Ni	0.04	0.06	0.00	0.00	0.06	0.05	0.29	0.20	0.24	0.05	0.01
Fe	0.98	0.39	0.90	0.85	0.51	0.71	0.84	0.31	0.30	0.70	0.64
Cu	0.13	0.08	0.15	0.07	0.05	0.23	0.17	0.10	0.14	0.01	0.81
S	30.29	33.55	30.99	32.78	32.90	34.59	34.62	35.17	35.21	35.85	33.17
As	4.22	0.00	1.54	0.71	0.02	0.47	0.48	0.00	0.00	0.28	0.59
Total	101.76	99.16	98.22	98.66	99.28	99.69	100.92	100.68	100.94	98.86	100.11
At. prop.											
Os	0.206	0.193	0.166	0.155	0.246	0.086	0.162	0.132	0.140	0.023	0.197
Ir	0.098	0.042	0.133	0.078	0.036	0.063	0.067	0.105	0.064	0.016	0.045
Ru	0.638	0.767	0.683	0.755	0.713	0.834	0.723	0.705	0.739	0.933	0.719
Rh	0.059	0.006	0.018	0.014	0.008	0.022	0.015	0.025	0.043	0.053	0.029
Pt	0.000	0.000	0.000	0.000	0.000	0.000	0.000	0.000	0.000	0.000	0.000
Pd	0.005	0.000	0.002	0.002	0.000	0.001	0.000	0.001	0.000	0.004	0.003
Ni	0.001	0.002	0.000	0.000	0.002	0.002	0.009	0.006	0.007	0.001	0.000
Fe	0.034	0.013	0.032	0.029	0.017	0.023	0.028	0.010	0.010	0.022	0.022
Cu	0.004	0.002	0.005	0.002	0.002	0.006	0.005	0.003	0.004	0.000	0.024
ΣMetal	1.045	1.025	1.039	1.035	1.024	1.037	1.009	0.987	1.007	1.052	1.039
S	1.844	1.975	1.920	1.947	1.975	1.952	1.979	2.013	1.993	1.941	1.946
As	0.110	0.000	0.041	0.018	0.001	0.011	0.012	0.000	0.000	0.007	0.015
ΣAnion	1.955	1.975	1.961	1.965	1.976	1.963	1.991	2.013	1.993	1.948	1.961
Total	3.000	3.000	3.000	3.000	3.000	3.000	3.000	3.000	3.000	3.000	3.000